

Ciliary transport regulates PDGF-AA/ $\alpha\alpha$ signaling via elevated mammalian target of rapamycin signaling and diminished PP2A activity

Nicole L. Umberger^{a,b} and Tamara Caspary^b

^aGenetics and Molecular Biology Graduate Programs and ^bDepartment of Human Genetics, Emory University School of Medicine, Atlanta, GA 30322

ABSTRACT Primary cilia are built and maintained by intraflagellar transport (IFT), whereby the two IFT complexes, IFTA and IFTB, carry cargo via kinesin and dynein motors for anterograde and retrograde transport, respectively. Many signaling pathways, including platelet-derived growth factor (PDGF)-AA/ $\alpha\alpha$, are linked to primary cilia. Active PDGF-AA/ $\alpha\alpha$ signaling results in phosphorylation of Akt at two residues: P-Akt^{T308} and P-Akt^{S473}, and previous work showed decreased P-Akt^{S473} in response to PDGF-AA upon anterograde transport disruption. In this study, we investigated PDGF-AA/ $\alpha\alpha$ signaling via P-Akt^{T308} and P-Akt^{S473} in distinct ciliary transport mutants. We found increased Akt phosphorylation in the absence of PDGF-AA stimulation, which we show is due to impaired dephosphorylation resulting from diminished PP2A activity toward P-Akt^{T308}. Anterograde transport mutants display low platelet-derived growth factor receptor (PDGFR) α levels, whereas retrograde mutants exhibit normal PDGFR α levels. Despite this, neither shows an increase in P-Akt^{S473} or P-Akt^{T308} upon PDGF-AA stimulation. Because mammalian target of rapamycin complex 1 (mTORC1) signaling is increased in ciliary transport mutant cells and mTOR signaling inhibits PDGFR α levels, we demonstrate that inhibition of mTORC1 rescues PDGFR α levels as well as PDGF-AA-dependent phosphorylation of Akt^{S473} and Akt^{T308} in ciliary transport mutant MEFs. Taken together, our data indicate that the regulation of mTORC1 signaling and PP2A activity by ciliary transport plays key roles in PDGF-AA/ $\alpha\alpha$ signaling.

Monitoring Editor

Monica Bettencourt-Dias
Instituto Gulbenkian de Ciência

Received: May 1, 2014

Revised: Oct 31, 2014

Accepted: Nov 5, 2014

INTRODUCTION

Primary cilia, the microtubule-based projections found on the eukaryotic cell surface, are linked to a number of signaling pathways (Goetz and Anderson, 2010). Primary cilia are built and maintained by intraflagellar transport (IFT), whereby the two IFT complexes, IFTA and IFTB, carry cargo via kinesin and dynein motors

for anterograde and retrograde transport, respectively. Many signaling pathways, including Sonic hedgehog (Shh), Wnt, PDGF, and mammalian target of rapamycin complex 1 (mTORC1), are linked to primary cilia, because mutations in IFTA, IFTB, kinesins, or dyneins alter the signaling response (Huangfu *et al.*, 2003; Schneider *et al.*, 2005; Corbit *et al.*, 2008; Boehlke *et al.*, 2010). The relationship between IFT and signaling can be complex; for example, Shh response is reduced in IFTB, dynein, and kinesin mutants, but elevated in IFTA mutants (Huangfu *et al.*, 2003; May *et al.*, 2005; Tran *et al.*, 2008).

Altering IFT leads to distinct changes in ciliary structure, depending on which IFT or motor protein function is disrupted. For example, primary cilia do not form when anterograde transport is abolished via loss of IFTB or kinesin components. In contrast, cilia become swollen when either IFTA or dynein components are lost, preventing retrograde IFT (Goetz and Anderson, 2010). Several other classes of proteins play roles in trafficking and ciliary structure, including the small GTPase, ADP-ribosylation factor-like 13B (ARL13B; Larkins *et al.*, 2011). Loss of ARL13B disrupts the microtubule structure of

This article was published online ahead of print in MBoc in Press (<http://www.molbiolcell.org/cgi/doi/10.1091/mbc.E14-05-0952>) on November 12, 2014.

The authors have no conflicts to report.

Address correspondence to: Tamara Caspary (tcaspar@emory.edu).

Abbreviations used: ARL13B, ADP-ribosylation factor-like 13B; IF, immunofluorescence; IFT, intraflagellar transport; MEF, mouse embryonic fibroblast; mTORC1, mammalian target of rapamycin complex 1; OA, okadaic acid; PI3K, phosphatidylinositol 3 kinase; Shh, Sonic hedgehog; WB, Western blotting.

© 2015 Umberger and Caspary. This article is distributed by The American Society for Cell Biology under license from the author(s). Two months after publication it is available to the public under an Attribution-Noncommercial-Share Alike 3.0 Unported Creative Commons License (<http://creativecommons.org/licenses/by-nc-sa/3.0>).

"ASCB®," "The American Society for Cell Biology®," and "Molecular Biology of the Cell®" are registered trademarks of The American Society for Cell Biology.

primary cilia and the localization and distribution of proteins within cilia (Caspary *et al.*, 2007; Larkins *et al.*, 2011).

Distinct signaling pathways require cilia for their activity. The best characterized of these is Shh signal transduction, which does not occur in the absence of cilia; dynamic ciliary movement of the Shh receptor and other pathway components is necessary to elicit an Shh response (Corbit *et al.*, 2005; Haycraft *et al.*, 2005; May *et al.*, 2005; Rohatgi *et al.*, 2007). The relationship between PDGF signaling and cilia is less understood. PDGF-AA acts through PDGFR α homodimers to activate downstream targets, including Akt kinase. PDGFR α is up-regulated and enriched in primary cilia in growth-arrested fibroblasts (Schneider *et al.*, 2005), and PDGF-AA/ α signaling is critical to induce G₀ cells into the cell cycle (Stiles *et al.*, 1979; Pledger *et al.*, 1981; Greenberg and Ziff, 1983). Moreover, PDGF-AA cannot signal in fibroblasts lacking cilia, suggesting ciliary localization of the receptor may be critical to its function. However, cells lacking cilia display decreased PDGFR α protein levels, which could also explain the lowered signaling (Schneider *et al.*, 2005, 2010).

Akt is fully activated via phosphorylation of T308 (P-Akt^{T308}) and S473 phosphorylation (P-Akt^{S473}). Dephosphorylation of P-Akt^{T308} is mediated by the phosphatase PP2A. PP2A regulates the activity of a variety of additional substrates and is negatively regulated by the mammalian target of rapamycin complex 1 (mTORC1) (Andjelković *et al.*, 1996; Zhao *et al.*, 2003; Vereshchagina *et al.*, 2008; Boehlke *et al.*, 2010; McBride *et al.*, 2010; Jackson and Pallas, 2012). Interestingly, the activities of both Akt and mTORC1 are linked to primary cilia (Schneider *et al.*, 2005, 2010; Boehlke *et al.*, 2010; Clement *et al.*, 2013). Here, using mouse embryonic fibroblasts (MEFs) deficient for distinct aspects of ciliary transport, we investigate the role of ciliary transport in PDGF-AA/ α signaling along with the mechanistic connections to PP2A activity and mTORC1 signaling. Our data highlight the intricate connections among signaling pathways as they relate to cilia, emphasizing the role of the primary cilium as a signaling hub.

RESULTS

Abnormal response to PDGF-AA signaling in ciliary transport mutant MEFs

PDGF-AA/ α stimulation induces activation of Akt through phosphorylation on two residues, T308 and S473 (Bellacosa *et al.*, 1998). Previous work has shown that PDGF-AA stimulation fails to increase P-Akt^{S473} in *Ift88^{orpk}* MEFs carrying a hypomorphic mutation in the IFTB component (Schneider *et al.*, 2005, 2010). To investigate the role of additional ciliary transport proteins in PDGF-AA/ α signaling, including phosphorylation of both T308 and S473 residues, we derived control and mutant MEFs from mouse embryos carrying the following alleles of genes encoding ciliary proteins important for transport: *Ift172^{wim}* and *Ift172^{avc}*, an IFTB component involved in anterograde trafficking; *Ift122^{sopb}*, an IFTA component involved in retrograde trafficking; and *Arl13b^{hnn}*, a small, ciliary GTPase (Huangfu *et al.*, 2003; Caspary *et al.*, 2007; Friedland-Little *et al.*, 2011; Qin *et al.*, 2011). *Ift172^{wim}* and *Ift172^{avc}* represent null and hypomorphic alleles, respectively, in an IFTB complex protein, so *Ift172^{wim}* MEFs lack cilia, while *Ift172^{avc}* MEFs have truncated cilia; *Ift122^{sopb}* MEFs have disrupted retrograde transport and display swollen or bulgy cilia; and *Arl13b^{hnn}* MEFs have short cilia with an abnormal ultrastructure and mislocalized ciliary proteins. With the exception of *Ift172^{wim}* MEFs, which cannot form cilia, the other MEFs can be induced to form cilia through serum starvation. We grew control, *Ift172^{wim}*, *Ift172^{avc}*, *Ift122^{sopb}*, and *Arl13b^{hnn}* MEFs in serum-supplemented media until confluent, serum starved them for 48 h, stimulated them with PDGF-AA ligand, and then harvested the cells.

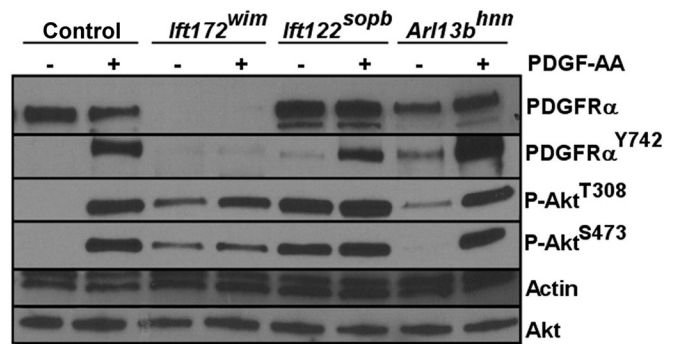


FIGURE 1: Response to PDGF-AA stimulation is misregulated in ciliary transport mutant MEFs. Comparison of PDGFR α , P-PDGFR α ^{Y742}, P-Akt^{T308}, and P-Akt^{S473} in control and ciliary transport mutant MEFs in the presence or absence of PDGF-AA ligand stimulation ($n = 3$).

We first examined PDGFR α levels in serum-starved control, *Ift172^{wim}*, *Ift122^{sopb}*, and *Arl13b^{hnn}* MEFs. Similar to the published results in *Ift88^{orpk}* MEFs, we found low PDGFR α levels in *Ift172^{wim}* MEFs, suggesting the phenotype is shared when IFTB components are disrupted (Figure 1). However, PDGFR α levels in *Ift122^{sopb}* and *Arl13b^{hnn}* MEFs are similar to control MEFs (Figure 1 and Supplemental Figure S1). We assessed phosphorylation of PDGFR α on Y742 (P-PDGFR α ^{Y742}), which occurs upon PDGF-AA binding to PDGFR α and initiates signaling (Yu *et al.*, 1991, 1994). In the absence of PDGF-AA stimulation, we found a slight elevation in basal levels of P-PDGFR α ^{Y742} in *Arl13b^{hnn}* and *Ift122^{sopb}* MEFs compared with control MEFs, indicating inappropriate activation of PDGFR α in the absence of PDGF-AA ligand (Figure 1 and Supplemental Figure S1). In response to PDGF-AA stimulation, we found P-PDGFR α ^{Y742} levels increased in control, *Arl13b^{hnn}*, and *Ift122^{sopb}* MEFs, while there was no P-PDGFR α ^{Y742} in *Ift172^{wim}* MEFs (Figure 1 and Supplemental Figure S1). Thus PDGFR α levels and response to PDGF-AA stimulation are disrupted in *Ift172^{wim}* anterograde mutants. In *Arl13b^{hnn}* and *Ift122^{sopb}* mutants, despite the slightly elevated basal P-PDGFR α ^{Y742}, the increase in P-PDGFR α ^{Y742} upon PDGF-AA stimulation indicates PDGFR α , when present, could be activated.

To measure downstream pathway activation, we analyzed both P-Akt^{T308} and P-Akt^{S473} levels in serum-starved control, *Ift172^{wim}*, *Ift122^{sopb}*, and *Arl13b^{hnn}* MEFs. We saw increased P-Akt^{T308} in all ciliary transport mutant MEFs compared with control MEFs, while P-Akt^{S473} was detectable only in *Ift172^{wim}* and *Ift122^{sopb}* MEFs (Figure 1 and Supplemental Figure S1). On PDGF-AA stimulation, we saw increased levels of P-Akt^{T308} and P-Akt^{S473} in control and *Arl13b^{hnn}* MEFs; however, there was no further increase in P-Akt^{T308} or P-Akt^{S473} levels upon PDGF-AA stimulation in *Ift172^{wim}* or *Ift122^{sopb}* MEFs (Figure 1 and Supplemental Figure S1). These data indicate that control and *Arl13b^{hnn}* MEFs respond to PDGF-AA by increasing phosphorylation of Akt, whereas *Ift172^{wim}* and *Ift122^{sopb}* MEFs do not. The insensitivity of P-Akt^{T308} or P-Akt^{S473} levels to PDGF-AA stimulation in *Ift172^{wim}* and *Ift122^{sopb}* MEFs is especially striking, because the mutations affected PDGFR α distinctly, pointing to PDGFR α -independent influences on either the phosphorylation or dephosphorylation of Akt.

P-Akt^{T308} is increased in ciliary transport mutant MEFs

Because Akt phosphorylation is stimulated through phosphoinositide 3-kinase (PI3K) signaling, we wanted to determine whether the increased P-Akt^{T308} levels were PI3K-dependent by treating the

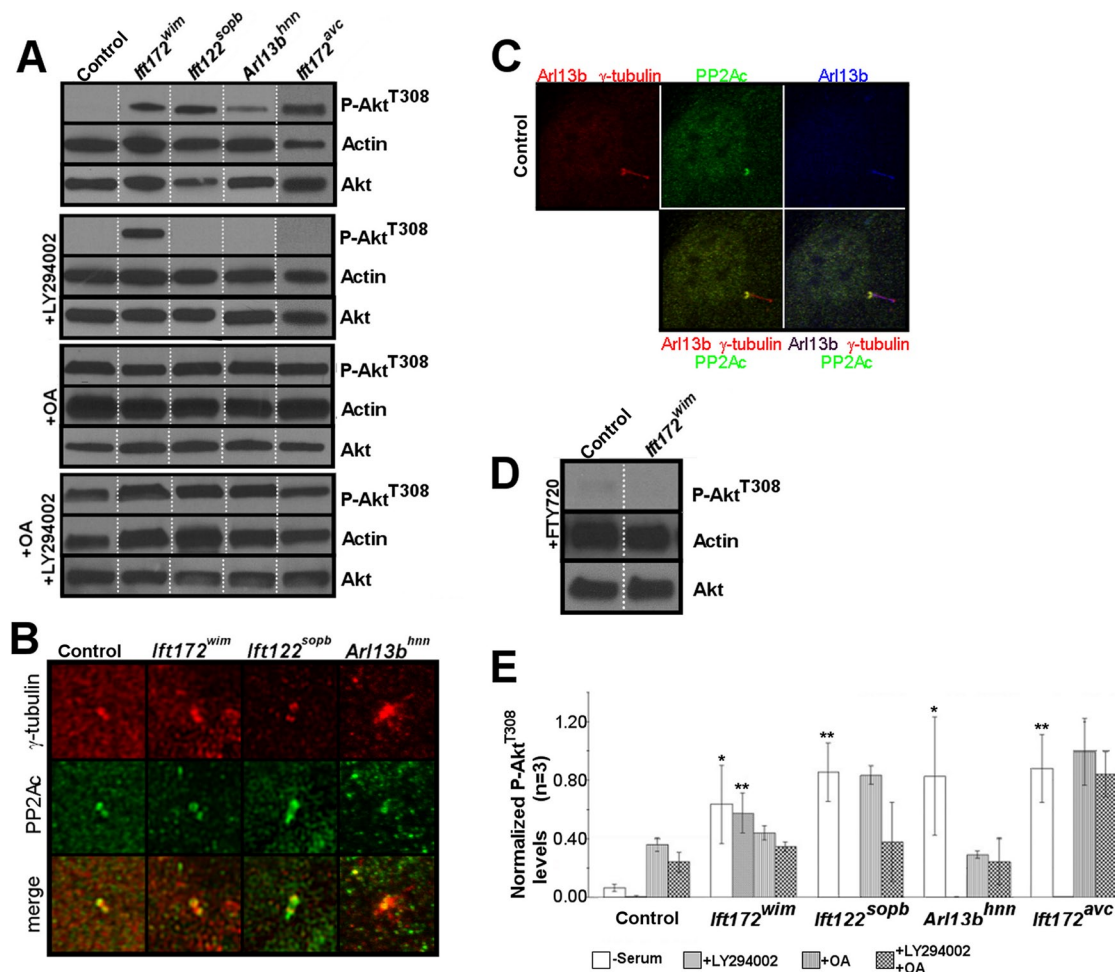


FIGURE 2: P-Akt^{T308} is increased in ciliary transport mutant MEFs and the P-Akt^{T308} phosphatase component PP2A localizes to the basal body. (A) Serum-starved control and ciliary transport mutant MEFs were lysed and processed for Western blot analysis of P-Akt^{T308} under the indicated experimental conditions (no serum, +LY294002, +OA, and +OA +LY294002). Note the presence of P-Akt^{T308} in *lft172^{wim}* MEFs during LY294002 treatment. Lanes shown are rearranged from a single gel. (B) Serum-starved control and ciliary transport mutant MEFs were immunolabeled for the catalytic subunit of PP2A PP2Ac (green) and for the basal body using γ -tubulin (red). (C) Serum-starved control MEFs were immunolabeled for the catalytic subunit of PP2A PP2Ac (green), for the basal body using γ -tubulin (red), and for cilia using Arl13b (red and blue). (D) Serum-starved control and *lft172^{wim}* MEFs were treated with a PP2A agonist, FTY720, and then lysed and processed for Western blot analysis of P-Akt^{T308}. FTY720 agonizes PP2A activity by inhibiting the PP2A inhibitor I2PP2A/SET1. Note the absence of P-Akt^{T308} in *lft172^{wim}* MEFs. (E) Average densitometry values of P-Akt^{T308} in control and ciliary transport mutant MEFs under the different experimental conditions. Error bars show SD ($n = 3$). Ciliary transport mutants were compared with their respective control littermates, under the same treatments, for statistical analyses ($n = 3$; *, $p < 0.05$; **, $p < 0.01$).

ciliary transport mutant MEFs with the PI3K inhibitor LY294002 (Andjelković *et al.*, 1996). We could not detect P-Akt^{T308} in LY294002-treated control, *lft172^{avc}*, *lft122^{sopb}*, or *Arl13b^{hnn}* MEFs, confirming the T308 phosphorylation we saw was PI3K dependent (Figure 2, A and E). Notably, P-Akt^{T308} remained elevated in *lft172^{wim}* MEFs after LY294002 treatment (Figure 2, A and E). This could be due either to a PI3K-independent pathway phosphorylating P-Akt^{T308} or to a lack of P-Akt^{T308} dephosphorylation.

PP2Ac localizes to the basal body of MEFs

PP2A, a serine-threonine phosphatase, regulates the activity of Akt by dephosphorylating Akt on T308 and localizes to the flagella of *Chlamydomonas reinhardtii* (Yang *et al.*, 2000). PP2A also localizes to the centrosome of mammalian cells (Horn *et al.*, 2007; Flegg *et al.*,

2010). The localization of PP2A relative to vertebrate cilia is unknown, so we first sought to determine the localization of PP2A relative to the cilium in serum-starved, control MEFs. To do so, we costained control MEFs with γ -tubulin and Arl13b and with an antibody for the catalytic subunit of PP2A (PP2Ac), and found PP2Ac localized to the basal body (Figure 2, B and C). Because P-Akt^{S473} and Akt^{T308} also localize to the basal body of ciliated cells (Zhu *et al.*, 2009; Schneider *et al.*, 2010), we examined P-Akt^{T308} localization relative to cilia and found P-Akt^{T308} localized to a single centriole of the basal body of control MEFs (Supplemental Figure S2). Notably, we saw no change in PP2Ac or P-Akt^{T308} localization at the basal body when we examined serum-starved ciliary transport mutant MEFs (Figure 2B and Supplemental Figure S1). Thus PP2Ac and its substrate, P-Akt^{T308}, localize to the basal body of ciliated control and ciliary transport mutant MEFs.

PP2A activity toward P-Akt^{T308} is disrupted in *Ift172^{wim}* mutant MEFs

To determine whether the loss of P-Akt^{T308} seen in control, *Ift172^{avc}*, *Ift122^{supb}*, and *Arl13b^{hnn}* MEFs after LY294002 treatment is PP2A dependent, we pharmacologically inhibited PP2A. Okadaic acid (OA) is a PP2A inhibitor, and treatment with OA increases P-Akt^{T308} in a variety of cell lines in vitro (Cohen et al., 1989; Edelstein and Rockwell, 2012; Li et al., 2013). If PP2A is responsible for the loss of P-Akt^{T308}, then treatment with LY294002 and OA should lead to increased P-Akt^{T308}. We performed our analysis in the presence of OA alone or in the presence of both OA and LY294002. Under either treatment, we detected P-Akt^{T308} in control, *Ift172^{wim}*, *Ift172^{avc}*, *Ift122^{supb}*, and *Arl13b^{hnn}* MEFs (Figure 2, A and E), indicating that disruption of PP2A activity can lead to increased P-Akt^{T308} levels, even in the absence of PI3K signaling.

The observations that P-Akt^{T308} is increased in the absence of serum but lost during PI3K inhibition indicate that dephosphorylation of P-Akt^{T308} is disrupted but still functional in *Ift172^{avc}*, *Ift122^{supb}*, and *Arl13b^{hnn}* MEFs. The observation that P-Akt^{T308} is increased in *Ift172^{wim}* MEFs even during PI3K inhibition suggests that dephosphorylation of P-Akt^{T308} is more severely impaired compared with the other ciliary transport mutants. Additionally, there may be aberrant signaling through other PI3K-independent pathways in the ciliary transport mutant MEFs that could contribute to the increased P-Akt^{T308}. However, as PP2A is localized to the basal body of ciliated MEFs, we propose that disruption of ciliary transport affects PP2A activity toward P-Akt^{T308}.

PP2A activity is regulated by endogenous inhibitors, such as I2PP2A/SET, which localizes to primary cilia in human retinal pigment epithelial cells (Li et al., 1996; Wang and Brautigan, 2008; Saddoughi et al., 2013). To directly test whether loss of PP2A activity is responsible for the persistence of P-Akt^{T308} in *Ift172^{wim}* MEFs, we treated the cells with FTY720, the inhibitor of I2PP2A/SET, which thereby functioned as a PP2A agonist. We found P-Akt^{T308} levels in *Ift172^{wim}* MEFs with FTY720 treatment were equivalent to those in control MEFs, indicating that the defect in *Ift172^{wim}* MEFs is due to lack of PP2A activity (Figure 2D). Taken together, our data argue that lack of anterograde transport, as in *Ift172^{wim}* MEFs, results in an absence of PP2A activity, whereas diminished anterograde transport, as in the *Ift172^{avc}* MEFs, or abnormal transport, as in the *Ift122^{supb}* and *Arl13b^{hnn}* MEFs, leads to decreased PP2A activity (Figure 2E).

Additionally, we examined *Dync2h1^{ln}* MEFs, which carry a null allele of the retrograde dynein motor. *Dync2h1^{ln}* MEFs do not survive in serum-free conditions, requiring us to grow the cells in 0.5% serum, which introduces confounding signaling (Ocbina and Anderson, 2008; Ocbina et al., 2011; Supplemental Figure S3A). Nevertheless, P-Akt^{T308} was absent following PI3K inhibition (LY294002) and present following PP2A inhibition (OA) (Supplemental Figure S3A). We investigated the *Dync2h1^{ln}* MEFs in all subsequent assays and found the results were consistent with results from *Ift122^{supb}*, the other mutant that primarily affects retrograde transport (Supplemental Figure S2). Because *Ift122^{supb}* cells grow in the absence of sera, we focused on them.

Total PP2A activity is similar in control and ciliary transport mutant MEFs

PP2A has dozens of substrates that belong to a variety of pathways (Andjelković et al., 1996; Janssens and Goris, 2001; Vereshchagina et al., 2008; Basu, 2011). To determine whether overall PP2A activity is altered in the ciliary transport mutant MEFs, we used two distinct assays: 1) a commercially available PP2A activity assay; and 2) Western blot analysis of the inactive, unmethylated PP2A pool.

For the phosphatase activity assay, PP2A was immunoprecipitated from the cell lysates and its activity monitored on a specific phosphopeptide substrate (K-R-pT-I-R-R; Saddoughi et al., 2013). While our control showed reduced PP2A activity by inhibition with OA in control and ciliary transport mutant lysates (Figure 3A), we found no difference in PP2A activity toward the phosphopeptide in any of the ciliary transport mutant MEFs compared with control MEFs. For the second assay, we monitored the methylation state of PP2Ac. Active PP2Ac is methylated, so unmethylated PP2Ac represents inactive PP2A (Turowski et al., 1995; Jackson and Pallas, 2012). We measured both total and unmethylated PP2Ac expression by Western blotting and found no differences in the level of total or unmethylated PP2Ac expression in control, *Ift172^{wim}*, *Ift122^{supb}*, or *Arl13b^{hnn}* MEFs (Figure 3B). These data indicate that ciliary transport does not alter overall PP2A activity and suggest that a subset of PP2A activity is affected.

mTORC1 pathway activity is increased in ciliary transport mutant MEFs

mTORC1 signaling and PP2A negatively regulate one another, and loss of cilia can result in increased mTORC1 signaling (Ballou et al., 1988; Peterson et al., 1999; Petritsch et al., 2000; Boehlke et al., 2010; Li et al., 2013). Thus we wanted to determine whether mTORC1 signaling is increased in the ciliary transport mutant MEFs. We assayed mTORC1 pathway activity by monitoring phosphorylation of the mTORC1 subunit, mTOR (P-mTOR^{S2448}), and mTORC1's substrate, p70 S6K (P-p70 S6K^{T389}), through Western analysis. mTOR is the core component of mTORC1 and is phosphorylated on S2448 (P-mTOR^{S2448}) via Akt signaling (Inoki et al., 2002). Active mTORC1 phosphorylates p70 S6K (P-p70 S6K^{T389}; Ballou, 1988; Jeno, 1988; Ferrari et al., 1991; Burnett et al., 1998; Isotani et al., 1999). Notably, P-p70 S6K^{T389} is a PP2A substrate (Ballou et al., 1988). We found elevated expression of P-mTOR^{S2448} and of P-p70 S6K^{T389} in *Ift172^{wim}*, *Ift172^{avc}*, *Ift122^{supb}*, and *Arl13b^{hnn}* MEFs compared with control MEFs, indicating mTORC1 signaling is up-regulated when ciliary transport is disrupted (Figure 4A).

Rapamycin treatment restores PDGFR α levels and response to PDGF-AA stimulation

mTORC1 signaling can also inhibit PDGFR α levels, thereby decreasing PDGF-AA/ $\alpha\alpha$ signaling (Zhang et al., 2003, 2007). To test whether the aberrant PDGF-AA response in *Ift172^{wim}* MEFs was the result of increased mTORC1 inhibiting PDGFR α levels, we treated the cells with the mTORC1 inhibitor rapamycin and examined PDGFR α expression and PDGF-AA response. We first showed that rapamycin is able to inhibit mTORC1 signaling, with or without PDGF-AA, in wild-type and ciliary transport mutant MEFs (Supplemental Figure S4D). Despite an absence of cilia (Supplemental Figure S4C), we found total PDGFR α expression levels, by Western blotting, were restored by rapamycin in *Ift172^{wim}* MEFs (Figure 4C; compare with Figure 1 and Supplemental Figure S1). While PDGFR α is localized to the cilia of serum-starved wild-type MEFs, we did not see distinct regions of PDGFR α staining in *Ift172^{wim}* MEFs, with or without rapamycin (Supplemental Figure S4). We also saw induction of P-PDGFR α ^{Y742}, P-Akt^{T308}, and P-Akt^{S473} expression upon PDGF-AA stimulation, indicating that limited PDGFR α levels could explain the low PDGF-AA/ $\alpha\alpha$ response of IFT mutants (Figure 4C; compare with Figure 1).

The increased basal P-Akt^{T308} in rapamycin-treated control MEFs highlights the feedback among mTORC1 signaling, PP2A activity, and PDGF-AA/ $\alpha\alpha$ signaling. P-Akt^{T308} levels reflect the

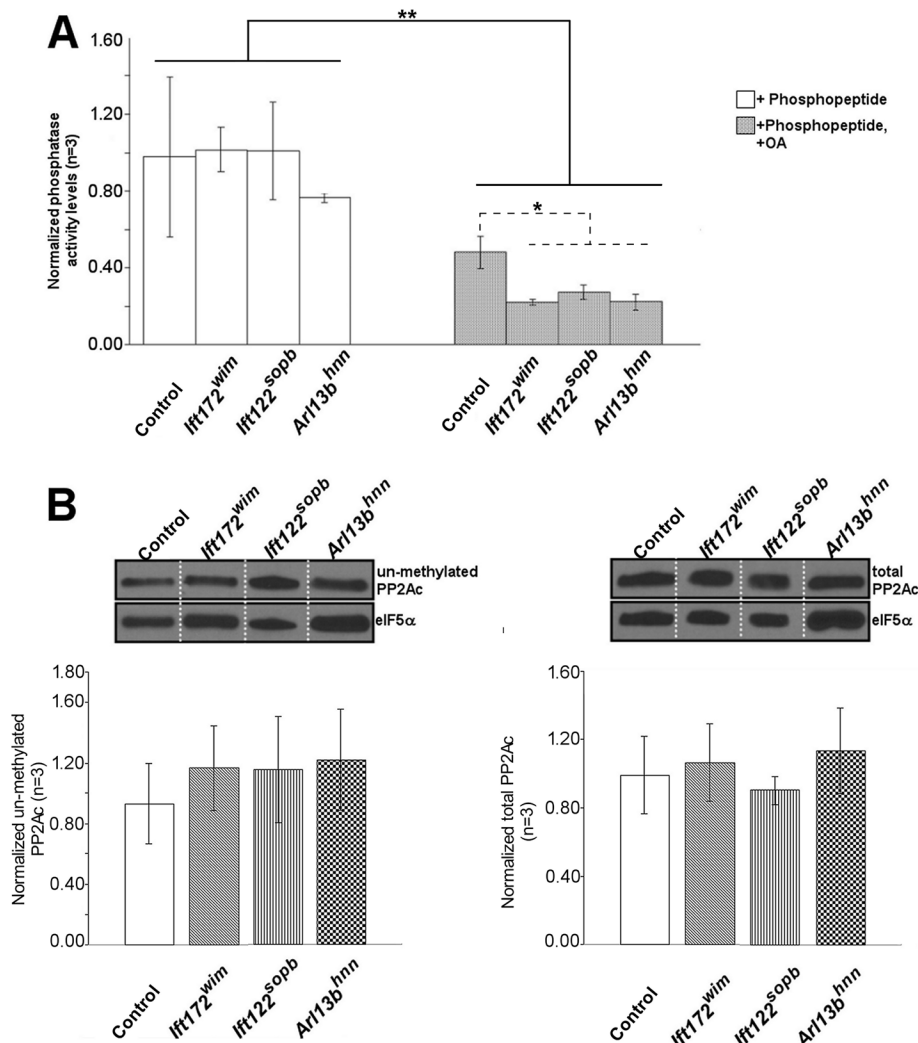


FIGURE 3: PP2A phosphatase activity and levels of total and unmethylated PP2Ac are unchanged in ciliary transport mutant MEFs. (A) PP2A activity was measured in control and ciliary transport mutant MEFs. Bars show the average of three independent experiments. Error bars show SD ($n = 3$; *, $p < 0.05$; **, $p < 0.01$). (B) Serum-starved control and ciliary transport mutant MEFs were lysed and processed for Western blot analysis of total and unmethylated PP2Ac levels. Lanes shown are rearranged from a single gel. Bar graphs show average densitometry values of unmethylated and total PP2Ac of control and ciliary transport mutant MEFs ($n = 3$).

relative activities of PDGF-AA/ α -induced phosphorylation of Akt and of PP2A-mediated dephosphorylation of Akt. Previous reports showed that rapamycin can induce Akt phosphorylation (because loss of mTORC1 signaling increases PDGFR α protein expression and downstream signaling) and can increase PP2A activity (via loss of mTORC1's inhibition of PP2A) (Rodrik-Outmezguine *et al.*, 2011; Ho *et al.*, 2012; Li *et al.*, 2013). Indeed, when we treated control MEFs with rapamycin and increasing concentrations of PDGFR α blocking antibody and then stimulated with PDGF-AA, the P-Akt^{T308} levels dropped as PDGFR α blocking antibody concentration increased (Figure 4, D and E). We next tested whether the feedback equilibrium depends on IFT172 by repeating this treatment regimen in *Ift172^{wim}* MEFs. We found that P-Akt^{T308} levels were unchanged in *Ift172^{wim}* MEFs in contrast to control MEFs (Figure 4, D and E). Together these data argue that the role of mTORC1 signaling in regulating the phosphorylation of Akt via PDGF-AA/ α signaling and PP2A activity depends on Ift172.

AA/ α signaling. Consistent with this, the other ciliary transport mutants also showed restoration of PDGF-AA/ α response (measured by increased P-Akt levels) upon rapamycin treatment, suggesting the lack of response in the ciliary transport mutants is due to elevated mTOR signaling.

Our finding of abnormally elevated P-Akt^{T308} levels in MEFs with aberrant ciliary transport indicates disrupted PP2A activity toward P-Akt^{T308}, with the most severe defects in MEFs deficient for anterograde transport (*Ift172^{wim}*). Indeed, in the presence of the PI3K inhibitor LY294002, the anterograde mutants show P-Akt^{T308} levels consistent with complete inhibition of PP2A activity; however, these cells do lack cilia, making it impossible to distinguish whether the lack of cilia or the absence of anterograde traffic underlies the diminished PP2A activity. In the remaining ciliary transport mutant MEFs, PP2A is active, albeit less efficient than in control. In fact, *Ift172^{avc}*, *Ift122^{sopb}*, *Arl13b^{hnn}*, and *Dync2h1^{ln}* MEFs required PI3K inhibition for T308 to be completely dephosphorylated as in control MEFs.

DISCUSSION

In this paper, we extend our understanding of the links between cilia and PDGF-AA/ α signaling by investigating two phosphorylation sites known to activate Akt in the context of distinct ciliary transport mutations. Consistent with previous data, we found low levels of P-Akt^{S473} when anterograde transport is disrupted (Schneider *et al.*, 2005, 2010). Moreover, we found that when either anterograde or retrograde ciliary transport is disrupted, both P-Akt^{T308} and P-Akt^{S473} levels are insensitive to PDGF-AA stimulation. Through pharmacological manipulation, we found that the aberrant P-Akt^{T308} results from problems with its dephosphorylation due to decreased PP2A activity, indicating that ciliary transport regulates a subset of PP2A activity. Defects in ciliary transport are linked to increased mTORC1 signaling, which is also known to inhibit both PP2A activity and PDGFR α protein levels. By inhibiting mTORC1 signaling, we restored PDGFR α protein levels in cells lacking cilia and rescued the PDGF-AA ligand response in cells deficient in ciliary transport. Thus our work reveals that ciliary transport regulates PDGF-AA/ α signaling through elevated mTOR signaling and diminished PP2A activity.

PDGFR α is up-regulated and enriched in primary cilia in growth-arrested fibroblasts (Lih *et al.*, 1996; Schneider *et al.*, 2005), and PDGF-AA/ α signaling is critical to induce G₀ cells into the cell cycle (Stiles *et al.*, 1979; Pledger *et al.*, 1981; Greenberg and Ziff, 1983). Because PDGF-AA/ α response is restored in rapamycin-treated MEFs lacking cilia (*Ift172^{wim}*), this implies that PDGFR α , although normally localized to cilia in vitro, need not be there to function. Such a model posits that cilia provide a site for efficient PDGF-AA/ α signaling and that functional ciliary transport helps fine-tune PDGF-

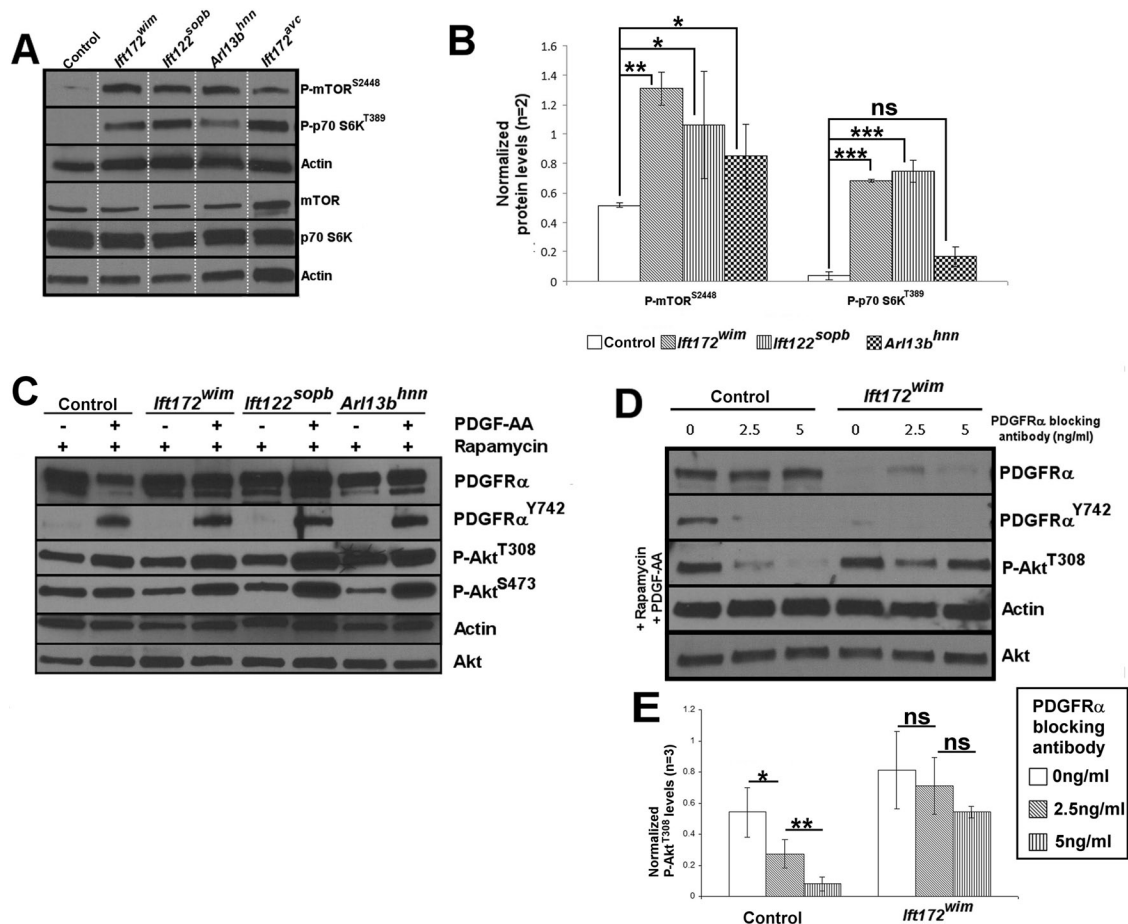


FIGURE 4: mTORC1 signaling is increased in ciliary transport mutant MEFs, and response to PDGF-AA stimulation is restored by rapamycin treatment. (A) Phosphorylation of mTOR (P-mTOR^{S2448}) ($n = 2$; control vs. *lft172^{wim}*; $p < 0.01$; control vs. *lft172^{sob}* and control vs. *Arl13b^{hnn}*; $p < 0.05$) and of p70 S6K (P-p70 S6K^{T389}) ($n = 2$; control vs. *lft172^{wim}* and control vs. *lft172^{sob}*; $p < 0.001$; control vs. *Arl13b^{hnn}*; $p = 0.0587$) are increased in ciliary transport mutant MEFs. Lanes shown are rearranged from a single gel. (B) Average densitometry values of P-mTOR^{S2448} and P-p70 S6K^{T389} in control and ciliary transport mutant MEFs. Error bars show SD (*, $p < 0.05$; **, $p < 0.01$; ***, $p < 0.001$). (C) Rapamycin treatment of control and ciliary transport mutant MEFs in the absence of serum, with or without PDGF-AA ligand stimulation. (D) P-Akt^{T308} levels of control and *lft172^{wim}* MEFs treated with rapamycin, PDGF-AA and an increasing concentration of PDGFR α blocking antibody ($n = 3$). (E) Average densitometry values of P-Akt^{T308} of control and *lft172^{wim}* MEFs treated with rapamycin, PDGF-AA, and an increasing concentration of PDGFR α blocking antibody ($n = 3$; *, $p < 0.05$; **, $p < 0.01$).

Our data show that total PP2A activity is not changed, suggesting that the effects on P-Akt^{T308} levels are due to misregulation of a specific pool of PP2A. We cannot pinpoint an exact mechanism for this—perhaps PP2A activity is affected only in specific subcellular compartments or perhaps only specific holoenzyme combinations of PP2A are affected. Several ciliary transport proteins, including *Arl13b*, can function outside the cilium, so perhaps they regulate PP2A activation in such a specific location (Robert *et al.*, 2007; Sedmak and Wolfrum, 2010; Delaval *et al.*, 2011; Barral *et al.*, 2012; Casalou *et al.*, 2014). Nonetheless, if only a subset of PP2A activity is decreased, it would explain why P-Akt^{T308} is increased but total in vitro PP2A activity is not altered in the ciliary transport mutant MEFs. Given that PP2Ac and P-Akt^{T308} are both localized at the base of cilia, we examined their signal intensity in the ciliary transport mutants but were unable to see any changes. This could be due to the changes being below the level of detection, which seems unlikely, because we could observe the differences by Western blotting. Alternatively, PP2A and Akt are both constantly trafficked around the cell, so their activity state need not be linked to their physical pres-

ence at the ciliary base. Our data suggest ciliary transport regulates PP2A activity and the Akt substrate's presence at the ciliary base facilitates Akt regulation.

There are several possibilities to explain how ciliary transport regulates PP2A activity, but our present work does not address whether this is via a direct or an indirect mechanism. One direct model would be that PP2A subunits or the assembled holoenzyme may require ciliary transport for activation, either by being physically brought into the cilium for activation or by an activator being transported into the cilium. Our observation that PP2Ac remained at the basal body in all ciliary transport mutant MEFs suggests the entire holoenzyme is not transported into the cilium. Alternatively, it is possible that an inhibitor of PP2A activity is regulated by ciliary transport. The rescue of P-Akt^{T308} dephosphorylation in *lft172^{wim}* MEFs upon treatment with FTY720 is consistent with this possibility, because FTY720 inhibits an endogenous inhibitor of PP2A, I2PP2A/SET (Li *et al.*, 1996; Saddoughi *et al.*, 2013). I2PP2A/SET localizes to cilia in at least one cell type, suggesting that ciliary transport controls the kinetics of I2PP2A/SET inhibition of PP2A,

thereby regulating a subset of PP2A activity, which can lead to indirect misregulation of the pathways PP2A regulates. The LY294002 sensitivity of *Ift172^{avc}* MEFs compared with the insensitivity of *Ift172^{wim}* MEFs would be consistent with such a model, because it suggests that the kinetics of ciliary transport are critical in regulating PP2A activity.

The feed-forward and feedback loops between mTORC1, PDGF-AA/ $\alpha\alpha$, and PP2A highlight the intricate connections between these pathways and provide the scaffold upon which more indirect models can be built. It is worth noting that the pharmacological approaches we used shift the finely tuned balance among mTOR, PP2A, and PDGF-AA/ $\alpha\alpha$, but do not cleanly reset all the pathways in the context of the others. Thus our data raise but cannot answer the question of whether the primary defect in the ciliary transport mutants is the increase in mTORC1 signaling or the diminished PP2A activity. Indeed, we observed increased basal P-PDGFR α ^{Y742} in both *Arl13b^{hnn}* and *Ift122^{sopb}* MEFs, which disappeared upon rapamycin treatment. The most parsimonious model favors the notion that disruption of ciliary transport leads to deregulation of a subset of PP2A activity, which in turn indirectly increases mTORC1 signaling. Normally, mTORC1 signaling results in phosphorylation of p70 S6K^{T389}, and P-p70 S6K^{T389} is a PP2A substrate (Ballou *et al.*, 1988; Hahn *et al.*, 2010). Thus, diminished PP2A activity can explain the increased mTORC1 signaling and the aberrant P-Akt^{T308} levels we see in ciliary transport mutant MEFs.

An alternative model, that the increased mTORC1 signaling causes the decreased PP2A activity, predicts that total PP2A activity would be lowered. Because total PP2A activity is not decreased in *Ift172^{wim}* MEFs, where P-Akt^{T308} levels are elevated under multiple conditions, this model is less likely. Furthermore, experiments that manipulate ciliary transport or various PP2A subunits *in vivo* also indicate that other PP2A functions are spared in ciliary transport mutants. PP2A *C α ^{-/-}* embryos die around embryonic day 6.5 (e6.5) and fail to form mesoderm, underscoring the essential role of PP2A early in development (Götz *et al.*, 1998). In contrast, *Ift172^{wim}*, *Ift172^{avc}*, *Ift122^{sopb}*, *Arl13b^{hnn}*, and *Dync2h1^{ln}* embryos form mesoderm and survive through midgestation (Huangfu *et al.*, 2003; Caspary *et al.*, 2007; Ocbina and Anderson, 2008; Friedland-Little *et al.*, 2011; Qin *et al.*, 2011).

The past decade has witnessed a flurry of research into the primary cilium as a fundamental signaling organelle. Indeed, mutations in many cilia-related genes lead to the human ciliopathies, which are linked to diverse signaling pathways. Our data show that ciliary transport plays a role in the relationship among these pathways. Rescue of the PDGF-AA response in cells lacking cilia raise the possibility that some pathways localized in cilia may be there for efficiency; perhaps the cilium provides highly regulated real estate that facilitates pathway transduction. The next steps will distinguish between direct and indirect mechanisms for the relationships among the signal transduction pathways linked to cilia and will address when the receptors can and do act.

MATERIALS AND METHODS

Cell culture

Primary cultures of control, *Arl13b^{hnn}*, *Ift172^{wim}*, *Ift172^{avc}*, and *Ift122^{sopb}* mouse embryonic fibroblasts were isolated from e11.5–e12.5 embryos and maintained in DMEM/F12 supplemented with 10% heat-inactivated fetal bovine serum and 1% penicillin/streptomycin (Corning, Manassas, VA: 10-092). Control MEFs were wild-type or heterozygous for *Arl13b^{hnn}*, *Ift172^{wim}*, *Ift172^{avc}*, or *Ift122^{sopb}*, and were paired with their respective ciliary transport mutant littermates for experiments. Primary *Dync2h1^{ln}* and *Ift172^{avc}* MEFs were

provided by Kathryn Anderson (Memorial Sloan Kettering Cancer Center) and *Ift122^{sopb}* MEFs by Jonathan Eggenschwiler (University of Georgia). MEFs were grown until confluent on plates precoated with 0.1% gelatin and then serum starved for 48 h before lysis and processing for Western blot analysis. Ciliary transport mutant cells, except *Ift172^{wim}*, which lack cilia, were ciliated to roughly similar percentages, just below 20%. Depending on the experiment, cells were treated at the following doses/times: 50 ng/ml PDGF-AA for 10 min (R&D Systems, Minneapolis, MN: 221-AA); 50 μ M LY294002 for 1 h (Cell Signaling, Danvers, MA: 9901); 10 nM rapamycin for 24 h (MP Biomedicals, Santa Ana, California: 159346); 200 nM OA for 3 h (Cell Signaling: 5934); and FTY720 for 5 h (Sigma-Aldrich, St. Louis, MO: SML0700-5MG).

PP2A immunoprecipitation phosphatase assay

The kit was purchased from Millipore (17-313). Experiments were performed following the manufacturer's protocol with 500 μ g protein lysate, with or without 1 μ M OA (Cell Signaling: 5934) during the phosphopeptide incubation.

Immunofluorescence (IF)

MEFs were grown and prepared for IF as previously described (Larkins *et al.*, 2011). Fluorescence was visualized on either an Olympus FluoView 100 confocal IX81 inverted microscope, a Nikon Structured Illumination Microscope, or a Leica DM600B upright microscope. Images were processed using Fiji software (Schindelin *et al.*, 2012).

SDS-PAGE and Western blot analysis

MEFs were rinsed with cold phosphate-buffered saline, scraped off the plate with a cell scraper, and lysed in 150 μ l of RIPA buffer supplemented with protease and phosphatase inhibitors (Sigma-Aldrich: P5726; Roche: 1697498001 and 04906845001). For experiments examining demethylated PP2Ac, lysates were prepared as described below, along with an additional treatment to demethylate PP2Ac (Jackson and Pallas, 2012). MEF lysate was passed through a 25 $\frac{5}{8}$ gauge needle 10 times and spun down at 16,000 relative centrifugal force for 10 min at 4°C, after which the supernatant was transferred to a clean tube. Protein concentrations were determined with a BCA protein kit (Pierce, Rockford, IL: 23221) or by Coomassie blue staining. MEF lysates were mixed with loading buffer, separated by SDS-PAGE on 4–20% Mini-PROTEAN TGX Precast Gels (456-1096EDU) with SDS running buffer, and transferred to Trans-Blot Turbo nitrocellulose membranes (Bio-Rad: 170-4059) using the Trans-Blot Turbo system (Bio-Rad: 170-4155). Membranes were blocked for 10 min at room temperature and incubated with primary antibodies in blocking buffer (Pierce: 37538) overnight at 4°C. Primary antibodies were detected using horseradish peroxidase-conjugated secondary antibodies (GE Healthcare Life Sciences, Pittsburgh, PA; NA934, and NA931) in 5% wt/vol nonfat milk in 0.1% Tris buffered saline with 0.1% Tween (TBST) at room temperature for 1 h and visualized with Amersham ECL Prime (GE Healthcare Life Sciences: RPN2232). Within each experiment, samples are from the same blot, originally performed in duplicate or in triplicate, and edited to show one representative band for each experimental condition, with white dotted lines drawn between lanes for ease of viewing. Band intensities from two to three biological replicates per condition were measured with Fiji software and normalized to actin loading control before averaging (McLean and Bennett, 2013). Bar graphs show the average of two or three experimental bands (as indicated) normalized to actin, with error

bars showing SD. Data were analyzed using unpaired two-tailed *t* tests (Supplemental Table S1).

Antibodies

We used the following antibodies at the indicated dilutions for Western blotting (WB) or IF: from Cell Signaling, Akt (WB 1:1000, IF 1:200, #9272), P-Akt^{S473} (WB 1:1000, IF 1:500, #587F11), P-Akt^{T308} (WB 1:1000, IF 1:500, #2965), mTOR (WB 1:2000, #2983), P-mTOR^{S2448} (WB 1:2000, #5536), P70 S6K (WB 1:2000, #2708), P-P70 S6K^{S371} (WB 1:2000, #9208), S6 (WB 1:2000, #2217), and P-S6 (WB 1:2000, #2211). From BD Pharmingen (San Diego, CA), PDGFR α (IF 1:200, #558774). From Santa Cruz Biotech (Dallas, TX), PDGFR α (WB 1:1000). From Sigma-Aldrich, acetylated tubulin (IF 1:2500, #T6793), actin (WB 1:1000, #A5060), α -rabbit γ -tubulin (IF 1:1000, #T5192), α -mouse γ -tubulin (IF 1:1000, #T6557), and P-PDGFR α ^{Y742} (WB 1:1000, #P8246). PP2Ac antibody was kindly provided by David Pallas (Emory University; WB 1:10,000, IF 1:200; BD Transduction Laboratories: 610555).

ACKNOWLEDGMENTS

We thank Kathryn Anderson, Jonathan Eggenschwiler, and David Pallas for providing reagents; members of the Caspary lab for comments; and Cheryl Timms Strauss for editing. This research project was supported with research funding from the Muscular Dystrophy Association (131071), National Institute of Neurological Disorders and Stroke (NINDS; R01 NS056380), and Emory Neuroscience NINDS Core Facilities (P30NS055077—Emory University Integrated Cellular Imaging Microscopy Core). N.L.U. was supported by an Emory PRISM Graduate Teaching Fellows in K–12 Education Fellowship (DGE0536941), an Emory Genetics and Molecular Biology Graduate Program Training Grant (T32GM008490), and an Emory Human Disease Genetics Training Fellowship (T32MH087977).

REFERENCES

Andjelković M, Jakubowicz T, Cron P, Ming XF, Han JW, Hemmings BA (1996). Activation and phosphorylation of a pleckstrin homology domain containing protein kinase (RAC-PK/PKB) promoted by serum and protein phosphatase inhibitors. *Proc Natl Acad Sci USA* 93, 5699–5704.

Ballou LM (1988). S6 kinase in quiescent Swiss mouse 3T3 cells is activated by phosphorylation in response to serum treatment. *Proc Natl Acad Sci USA* 85, 7154–7158.

Ballou LM, Jenö P, Thomas G (1988). Protein phosphatase 2A inactivates the mitogen-stimulated S6 kinase from Swiss mouse 3T3 cells. *J Biol Chem* 263, 1188–1194.

Barral DC, Garg S, Casalou C, Watts GFM, Sandoval JL, Ramalho JS, Hsu VW, Brenner MB (2012). Arl13b regulates endocytic recycling traffic. *Proc Natl Acad Sci USA* 109, 21354–21359.

Basu S (2011). PP2A in the regulation of cell motility and invasion. *Curr Protein Pept Sci* 12, 3–11.

Bellacosa A, Chan TO, Ahmed NN, Datta K, Malstrom S, Stokoe D, McCormick F, Feng J, Tsichlis P (1998). Akt activation by growth factors is a multiple-step process: the role of the PH domain. *Oncogene* 17, 313–325.

Boehlke C, Kotsis F, Patel V, Braeg S, Voelker H, Bredt S, Beyer T, Janusch H, Hamann C, Gödel M, et al. (2010). Primary cilia regulate mTORC1 activity and cell size through Lkb1. *Nat Cell Biol* 12, 1115–1122.

Burnett PE, Barrow RK, Cohen NA, Snyder SH, Sabatini DM (1998). RAFT1 phosphorylation of the translational regulators p70 S6 kinase and 4E-BP1. *Proc Natl Acad Sci USA* 95, 1432–1437.

Casalou C, Seixas C, Portelinha A, Pintado P, Barros M, Ramalho JS, Lopes SS, Barral DC (2014). Arl13b and the non-muscle myosin heavy chain IIA are required for circular dorsal ruffle formation and cell migration. *J Cell Sci* 127, 2709–2722.

Caspary T, Larkins CE, Anderson KV (2007). The graded response to Sonic hedgehog depends on cilia architecture. *Dev Cell* 12, 767–778.

Clement DL, Mally S, Stock C, Lethan M, Satir P, Schwab A, Pedersen SF, Christensen ST (2013). PDGFR α signaling in the primary cilium regulates

NHE1-dependent fibroblast migration via coordinated differential activity of MEK1/2-ERK1/2-p90RSK and AKT signaling pathways. *J Cell Sci* 126, 953–965.

Cohen P, Klumpp S, Schelling DL (1989). An improved procedure for identifying and quantitating protein phosphatases in mammalian tissues. *FEBS Lett* 250, 596–600.

Corbit KC, Aanstad P, Singla V, Norman AR, Stainier DYS, Reiter JF (2005). Vertebrate Smoothed functions at the primary cilium. *Nature* 437, 1018–1021.

Corbit KC, Shyer AE, Dowdle WE, Gaulden J, Singla V, Chen M-H, Chuang P-T, Reiter JF (2008). Kif3a constrains beta-catenin-dependent Wnt signalling through dual ciliary and non-ciliary mechanisms. *Nat Cell Biol* 10, 70–76.

Delaval B, Bright A, Lawson ND, Doxsey S (2011). The cilia protein IFT88 is required for spindle orientation in mitosis. *Nat Cell Biol* 13, 461–468.

Edelstein J, Rockwell P (2012). Okadaic acid induces Akt hyperphosphorylation and an oxidative stress-mediated cell death in serum starved SK-N-SH human neuroblastoma cells that are augmented by rapamycin. *Neurosci Lett* 531, 74–79.

Ferrari S, Bandi HR, Hofsteenge J, Bussian BM, Thomas G (1991). Mitogen-activated 70K S6 kinase. Identification of in vitro 40 S ribosomal S6 phosphorylation sites. *J Biol Chem* 266, 22770–22775.

Flegg CP, Sharma M, Medina-Palazon C, Jamieson C, Galea M, Brocardo MG, Mills K, Henderson BR (2010). Nuclear export and centrosome targeting of the protein phosphatase 2A subunit B56 α : role of B56 α in nuclear export of the catalytic subunit. *J Biol Chem* 285, 18144–18154.

Friedland-Little JM, Hoffmann AD, Ocbina PJR, Peterson MA, Bosman JD, Chen Y, Cheng SY, Anderson K V, Moskowitz IP (2011). A novel murine allele of intraflagellar transport protein 172 causes a syndrome including VACTERL-like features with hydrocephalus. *Hum Mol Genet* 20, 3725–3737.

Goetz SC, Anderson K V (2010). The primary cilium: a signalling centre during vertebrate development. *Nat Rev Genet* 11, 331–344.

Götz J, Probst A, Ehler E, Hemmings B, Kues W (1998). Delayed embryonic lethality in mice lacking protein phosphatase 2A catalytic subunit C α . *Proc Natl Acad Sci USA* 95, 12370–12375.

Greenberg ME, Ziff EB (1983). Stimulation of 3T3 cells induces transcription of the *c-fos* proto-oncogene. *Nature* 311, 433–438.

Hahn K, Miranda M, Francis VA, Vendrell J, Zorzano A, Teleman AA (2010). PP2A regulatory subunit PP2A-B' counteracts S6K phosphorylation. *Cell Metab* 11, 438–444.

Haycraft CJ, Banizs B, Aydin-Son Y, Zhang Q, Michaud EJ, Yoder BK (2005). Gli2 and Gli3 localize to cilia and require the intraflagellar transport protein polaris for processing and function. *PLoS Genet* 1, e53.

Horn V, Thelu J, Garcia A, Albiges-Rizo C, Block MR, Viallet J (2007). Functional interaction of Aurora-A and PP2A during mitosis. *Mol Biol Cell* 18, 1233–1241.

Ho AL, Vasudeva SD, Laé M, Saito T, Barbashina V, Antonescu CR, Ladanyi M, Schwartz GK (2012). PDGF receptor alpha is an alternative mediator of rapamycin-induced Akt activation: implications for combination targeted therapy of synovial sarcoma. *Cancer Res* 72, 4515–4525.

Huangfu D, Liu A, Rakeman AS, Murcia NS (2003). Hedgehog signalling in the mouse requires intraflagellar transport proteins. *Nature* 426, 83–87.

Inoki K, Li Y, Zhu T, Wu J, Guan K-L (2002). TSC2 is phosphorylated and inhibited by Akt and suppresses mTOR signalling. *Nat Cell Biol* 4, 648–657.

Isotani S, Hara K, Tokunaga C, Inoue H, Avruch J, Yonezawa K (1999). Immunopurified mammalian target of rapamycin phosphorylates and activates p70 S6 kinase alpha in vitro. *J Biol Chem* 274, 34493–34498.

Jackson JB, Pallas DC (2012). Circumventing cellular control of PP2A by methylation promotes transformation in an Akt-dependent manner. *Neoplasia* 14, 585–599.

Janssens V, Goris J (2001). Protein phosphatase 2A: a highly regulated family of serine/threonine phosphatases implicated in cell growth and signalling. *Biochem J* 353, 417–439.

Jeno P (1988). Identification and characterization of a mitogen-activated s6 kinase. *Proc Natl Acad Sci USA* 85, 406–410.

Larkins CE, Aviles GDG, East MP, Kahn RA, Caspary T (2011). Arl13b regulates ciliogenesis and the dynamic localization of Shh signaling proteins. *Mol Biol Cell* 22, 4694–4703.

Li M, Makkinje A, Damuni Z (1996). The myeloid leukemia-associated protein SET is a potent inhibitor of protein phosphatase 2A. *J Biol Chem* 271, 11059–11062.

Li Y, Wang X, Yue P, Tao H, Ramalingam SS, Owonikoko TK, Deng X, Wang Y, Fu H, Khuri FR, et al. (2013). Protein phosphatase 2A and

- DNA-dependent protein kinase are involved in mediating rapamycin-induced Akt phosphorylation. *J Biol Chem* 288, 13215–13224.
- Lih CJ, Cohen SN, Wang C, Lin-Chao S (1996). The platelet-derived growth factor α -receptor is encoded by a growth-arrest-specific (*gas*) gene. *Proc Natl Acad Sci USA* 93, 4617–4622.
- May SR, Ashique AM, Karlen M, Wang B, Shen Y, Zarbalis K, Reiter J, Ericson J, Peterson AS (2005). Loss of the retrograde motor for IFT disrupts localization of Smo to cilia and prevents the expression of both activator and repressor functions of Gli. *Dev Biol* 287, 378–389.
- McBride SM, Perez DA, Polley MY, Vandenberg SR, Smith JS, Zheng S, Lamborn KR, Wiencke JK, Chang SM, Prados MD, et al. (2010). Activation of PI3K/mTOR pathway occurs in most adult low-grade gliomas and predicts patient survival. *J Neurooncol* 97, 33–40.
- McLean AC, Bennett SAL (2013). A protocol for densitometric quantification of Western blots using Image J [weblog entry]. Neural Regeneration Laboratory, Resources, University of Ottawa. Available at <http://137.122.232.177/resources.html>.
- Ocbina PJR, Anderson K V (2008). Intraflagellar transport, cilia, and mammalian Hedgehog signaling: analysis in mouse embryonic fibroblasts. *Dev Dyn* 237, 2030–2038.
- Ocbina PJR, Eggenschwiler JT, Moskowitz I, Anderson K V (2011). Complex interactions between genes controlling trafficking in primary cilia. *Nat Genet* 43, 547–553.
- Peterson RT, Desai BN, Hardwick JS, Schreiber SL (1999). Protein phosphatase 2A interacts with the 70-kDa S6 kinase and is activated by inhibition of FKBP12-rapamycin-associated protein. *Proc Natl Acad Sci USA* 96, 4438–4442.
- Petrtsch C, Beug H, Balmain A, Oft M (2000). TGF- β inhibits p70 S6 kinase via protein phosphatase 2A to induce G₁ arrest. *Genes Dev* 14, 3093–3101.
- Pledger WJ, Hart CA, Locatelli KL, Scher CD (1981). Platelet-derived growth factor-modulated proteins: constitutive synthesis by a transformed cell line. *Proc Natl Acad Sci USA* 78, 4358–4362.
- Qin J, Lin Y, Norman RX, Ko HW, Eggenschwiler JT (2011). Intraflagellar transport protein 122 antagonizes Sonic hedgehog signaling and controls ciliary localization of pathway components. *Proc Natl Acad Sci USA* 108, 1456–1461.
- Robert A, Margall-Ducos G, Guidotti J-E, Br gerie O, Celati C, Br chet C, Desdouets C (2007). The intraflagellar transport component IFT88/polaris is a centrosomal protein regulating G1-S transition in non-ciliated cells. *J Cell Sci* 120, 628–637.
- Rodrik-Outmezguine VS, Chandarlapaty S, Pagano NC, Poulidakos PI, Scaltriti M, Moskatel E, Baselga J, Guichard S, Rosen N (2011). mTOR kinase inhibition causes feedback-dependent biphasic regulation of AKT signaling. *Cancer Discov* 1, 248–259.
- Rohatgi R, Milenkovic L, Scott MP (2007). Patched1 regulates hedgehog signaling at the primary cilium. *Science* 317, 372–376.
- Saddoughi SA, Gencer S, Peterson YK, Ward KE, Mukhopadhyay A, Oaks J, Bielawski J, Szulc ZM, Thomas RJ, Selvam SP, et al. (2013). Sphingosine analogue drug FTY720 targets I2PP2A/SET and mediates lung tumour suppression via activation of PP2A-RIPK1-dependent necroptosis. *EMBO Mol Med* 5, 105–121.
- Schindelin J, Arganda-Carreras I, Frise E, Kaynig V, Longair M, Pietzsch T, Preibisch S, Rueden C, Saalfeld S, Schmid B, et al. (2012). Fiji: an open-source platform for biological-image analysis. *Nat Methods* 9, 676–682.
- Schneider L, Cammer M, Lehman J, Nielsen SK, Guerra CF, Veland IR, Stock C, Hoffmann EK, Yoder BK, Schwab A, et al. (2010). Directional cell migration and chemotaxis in wound healing response to PDGF-AA are coordinated by the primary cilium in fibroblasts. *Cell Physiol Biochem* 25, 279–292.
- Schneider L, Clement CA, Teilmann SC, Pazour GJ, Hoffmann EK, Satir P, Christensen ST (2005). PDGFR α signaling is regulated through the primary cilium in fibroblasts. *Curr Biol* 15, 1861–1866.
- Sedmak T, Wolfrum U (2010). Intraflagellar transport molecules in ciliary and nonciliary cells of the retina. *J Cell Biol* 189, 171–186.
- Stiles CD, Capone GT, Scher CD, Antoniades HN, Van Wyk JJ, Pledger WJ (1979). Dual control of cell growth by somatomedins and platelet-derived growth factor. *Proc Natl Acad Sci USA* 76, 1279–1283.
- Tran PV, Haycraft CJ, Besschetnova TY, Turbe-Doan A, Stottmann RW, Herron BJ, Chesebro AL, Qiu H, Scherz PJ, Shah JV, et al. (2008). THM1 negatively modulates mouse sonic hedgehog signal transduction and affects retrograde intraflagellar transport in cilia. *Nat Genet* 40, 403–410.
- Turowski P, Fernandez a, Favre B, Lamb NJ, Hemmings Ba (1995). Differential methylation and altered conformation of cytoplasmic and nuclear forms of protein phosphatase 2A during cell cycle progression. *J Cell Biol* 129, 397–410.
- Vereshchagina N, Ramel M-C, Bitoun E, Wilson C (2008). The protein phosphatase PP2A-B' subunit Widerborst is a negative regulator of cytoplasmic activated Akt and lipid metabolism in *Drosophila*. *J Cell Sci* 121, 3383–3392.
- Wang W, Brautigan DL (2008). Phosphatase inhibitor 2 promotes acetylation of tubulin in the primary cilium of human retinal epithelial cells. *BMC Cell Biol* 9, 62.
- Yang P, Fox L, Colbran RJ, Sale WS (2000). Protein phosphatases PP1 and PP2A are located in distinct positions in the *Chlamydomonas* flagellar axoneme. *J Cell Sci* 113, 91–102.
- Yu JC, Gutkind JS, Mahadevan D, Li W, Meyers KA, Pierce JH, Heidaran MA (1994). Biological function of PDGF-induced PI-3 kinase activity: its role in alpha PDGF receptor-mediated mitogenic signaling. *J Cell Biol* 127, 479–487.
- Yu JC, Heidaran MA, Pierce JH, Gutkind JS, Lombardi D, Ruggiero M, Aaronson SA (1991). Tyrosine mutations within the alpha platelet-derived growth factor receptor kinase insert domain abrogate receptor-associated phosphatidylinositol-3 kinase activity without affecting mitogenic or chemotactic signal transduction. *Mol Cell Biol* 11, 3780–3785.
- Zhang H, Bajraszewski N, Wu E, Wang H, Moseman AP, Dabora SL, Griffin JD, Kwiatkowski DJ (2007). PDGFRs are critical for PI3K/Akt activation and negatively regulated by mTOR. *J Clin Invest* 117, 730–738.
- Zhang H, Cicchetti G, Onda H, Koon HB, Asrican K, Bajraszewski N, Vazquez F, Carpenter CL, Kwiatkowski DJ (2003). Loss of Tsc1/Tsc2 activates mTOR and disrupts PI3K-Akt signaling through downregulation of PDGFR. *J Clin Invest* 112, 1223–1233.
- Zhao JJ, Gjoerup OV, Subramanian RR, Cheng Y, Chen W, Roberts TM, Hahn WC (2003). Human mammary epithelial cell transformation through the activation of phosphatidylinositol 3-kinase. *Cancer Cell* 3, 483–495.
- Zhu D, Shi S, Wang H, Liao K (2009). Growth arrest induces primary-cilium formation and sensitizes IGF-1-receptor signaling during differentiation induction of 3T3-L1 preadipocytes. *J Cell Sci* 122, 2760–2768.